



Modelling and Analysis of Inhomogeneous Back-to-Back Schottky Junction Diode

Norizam Saad^{1,2,*}, Shaharin Fadzli Abd Rahman^{3,*}, Abdul Manaf Hashim¹, Ishak Mansor²

¹ Malaysia–Japan International Institute of Technology (MJIIT), Universiti Teknologi Malaysia, Jalan Sultan Yahya Petra, 54100 Kuala Lumpur, Malaysia

² Technical Support Division, Malaysian Nuclear Agency, 43000 Kajang, Selangor, Malaysia

³ School of Electrical Engineering, Faculty of Engineering, Universiti Teknologi Malaysia, 81310 Johor Bahru, Johor, Malaysia

ARTICLE INFO

Article history:

Received 23 February 2024

Received in revised form 1 April 2024

Accepted 21 August 2024

Available online 19 September 2024

Keywords:

Schottky junction; inhomogeneous barrier; back-to-back diode; thermionic transport; current spreading

ABSTRACT

Back-to-back Schottky diode (BBS) is a simple device structure made from Schottky junctions that can be applied in various applications. In modelling and simulating the BBS, the inhomogeneity of the barrier height at the Schottky interface should be considered. This paper presents device models and simulation result of an inhomogeneous BBS. Two device models with different current spreading condition are considered. The distribution of the inhomogeneous barrier height is represented by Gaussian distribution. All the computation was done using Python programming software. When the standard deviation of the barrier height increases, the apparent barrier height that influence the electrical characteristic decreased. This is consistent with the reported experimental data. Device model that considers full current spreading showed 37.8% reduction of apparent barrier height at standard deviation of 100 meV. This is greater than the model with no current spreading. The ideality factor showed correlation with the standard deviation of barrier height, particularly when no current spreading is considered. At standard deviation of 100 meV, the ideality factor increased 2.6 %. The obtained non-unity ideality factor is associated to the significant fluctuation in the barrier height. The computed temperature-dependent current curves also showed good agreement with the reported experimental results. The device model can be a convenient tool to investigate the device operation and to validate the method used for extraction of Schottky barrier parameters.

1. Introduction

Selection of metal for electrode in semiconductor devices is important as the characteristics of the formed metal-semiconductor junction will influence the operation of the devices. For example, metal-semiconductor junction in source and drain electrodes of a transistor should show ohmic behaviour that enable current to flow in and out of the semiconductor substrate [1,2]. Metal-

* Corresponding author.

E-mail address: norizam@nuclearmalaysia.gov.my

* Corresponding author.

E-mail address: shaharinfadzli@utm.my

<https://doi.org/10.37934/araset.51.2.206214>

semiconductor junction can also restrict certain direction of current flow. This type of junction is called Schottky junction, and it exhibits rectifying behaviour as observed in PN junction diode [3]. The application of the Schottky junction in a diode enables fast switching at and low voltage, while in a transistor, the Schottky junction allows the modulation of current that flows along the channel [4,5]. The Schottky junction can also be found in the structure of electronic sensors [6]. Characterization of the Schottky junction properties such as barrier height is an important step to analyze and optimize the device operation. Carrier transport at the junction is described by the thermionic transport [7]. The current flow across the junction is determined by the amount of carrier that can overcome the Schottky barrier height at the metal-semiconductor interface.

Besides the barrier height, the ideality factor is another parameter that should be considered when analyzing the Schottky junction. The ideality factor is an indicator that shows how well the experimental result can be fitted to the ideal thermionic transport. In cases when the ideality factor is larger than unity, other carrier transport such as tunnelling may also contribute the current flow [8]. The non-unity ideality factor is also due to the inhomogeneity of the barrier height along the metal-semiconductor interface [9]. Factors such as process variation and unoptimized process parameter led to the fluctuation of the barrier height. Osvald [9] has proposed device models to investigate the effect of inhomogeneity.

This work focuses on a device structure called back-to-back Schottky diode (BBS) [10-13]. The fabrication of a normal Schottky diode structure requires the deposition of one Schottky electrode and one ohmic electrode onto the semiconductor substrate. As for BBS, both deposited electrodes are Schottky electrodes. In comparison to the normal Schottky diode, the BBS is fabricated through simpler process flow. When it is challenging to obtain a high-quality ohmic contact, the BBS is a practical alternative for accurate analysis of Schottky junction parameters [14-18]. The barrier inhomogeneity can be evaluated from the analysis of temperature-dependent apparent barrier height [10]. In the case of the BBS, the apparent barrier height is extracted using a modified thermionic transport equation [14]. The modification is made so that the ideality factor will have significant change to the reverse-bias current value.

The aim of this work is to employ the approach proposed by Osvald [9] for device modelling of the inhomogeneous BBS. The device model shall be used to understand the effect of current spreading and junction parameters such as barrier height fluctuation and temperature, to the current flow. Note that the ideality factor is not included in the device model. The model shall also give insight on how the barrier height inhomogeneity influences the ideality factor in the BBS's thermionic equation.

2. Device Models and Numerical Method

Figure 1(a) shows an example structure of the BBS. In the shown structure, the two Schottky electrodes are deposited on the same substrate surface. The BBS can also be a vertical BBS structure with top and bottom Schottky electrodes. For analysis of current-voltage characteristics of the BBS, the device can be modelled using the equivalent circuit shown in Figure 1(b) [10]. As the diodes are connected in opposite directions, when a voltage is applied (i.e., V_A), one diode is in forward-bias, and another one is in reversed-bias. Here, the right and left diodes are labelled as diode 1 (D1) and diode 2 (D2), respectively. I_{D1} is the current flows in D1 and I_{D2} is the current flows in D2. There is a resistor, R , connected in series with the diodes. The R represents series resistance that come from the substrate, electrodes, and electrical connections. Under the bias, the current at BBS can be computed by solving the following simultaneous equations.

$$V_{D1} + V_{D2} + I_{D1}R - V_A = 0 \quad (1)$$

$$V_{D1} + V_{D2} + I_{D2}R - V_A = 0 \quad (2)$$

V_{D1} and V_{D2} are the voltage drop at D1 and D2, respectively. I_{D1} is a current equation as a function of V_{D1} , while I_{D2} is a current equation as a function of V_{D2} .

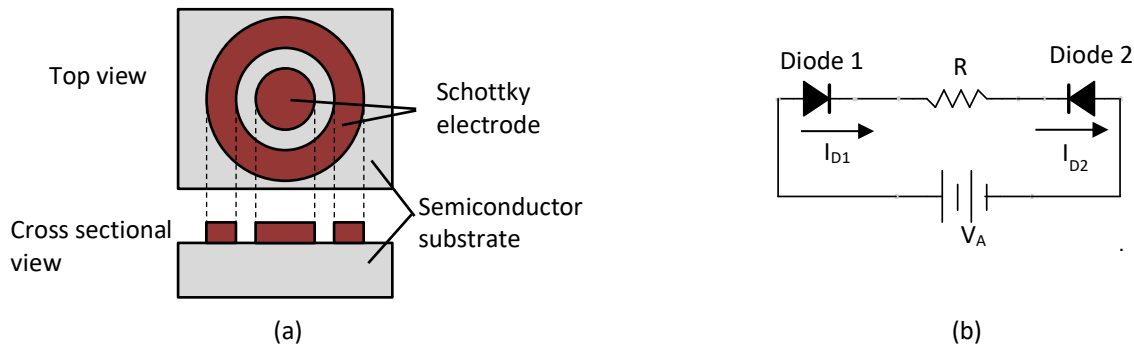


Fig. 1. (a) An example of BBSD structure (b) Equivalent circuit when applying V_A

In case of inhomogeneous Schottky junction, the Schottky junction can be segmented into units that possess different barrier height (ϕ_B). Figure 2 shows device model of the inhomogeneous BBSD. D1 and D2 are represented by multiple diodes connected in parallel. Diodes in the parallel connection have different ϕ_B . The distribution of the inhomogeneous ϕ_B is commonly described by a Gaussian distribution. The Gaussian probability density, ρ is given by the Eq. (3).

$$\rho = \frac{1}{\sigma_B \sqrt{2\pi}} \exp\left(-\frac{(\phi_B - \phi_{B,avg})^2}{2\sigma_B^2}\right) \quad (3)$$

σ_B is standard deviation of the barrier height and $\phi_{B,avg}$ is the mean barrier height. Osvald [9,19] have examined two conditions for inhomogeneous single Schottky diode. The first condition is when a complete current spreading is considered (i.e. model A). All the peripheral resistances are represented by one resistor. Another condition is when no current spreading is considered (i.e. model B). The current between the electrodes is due to the carrier movement along multiple parallel paths that connect both electrodes. In case of complete current spreading, the current at each current path is uniform. Thus, the resistance of the current paths can be represented by one resistor. On the other hand, in case of no current spreading, certain parallel path may have significantly low resistance than other current paths. The current spreading in the device depends on multiple factors such as device geometry and material conductivity [20].

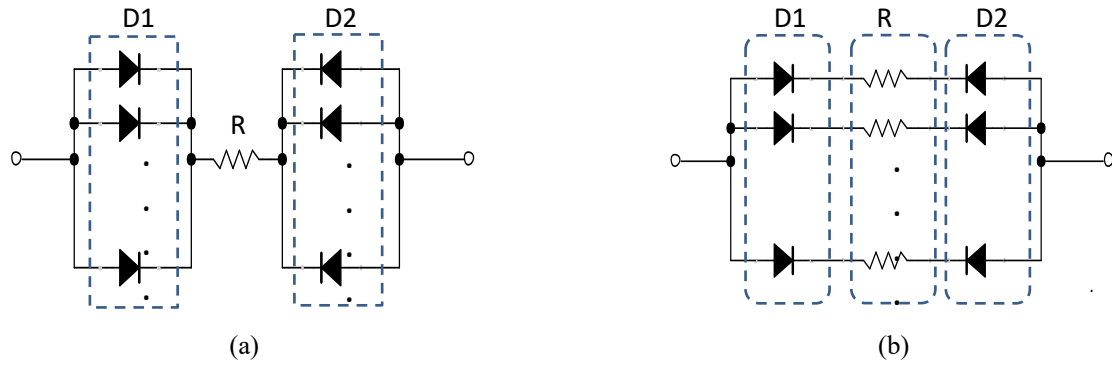


Fig. 2. Equivalent device model of inhomogeneous BBSD with consideration of (a) Complete current spreading (model A) (b) No current spreading (model B)

To solve the device model A shown in Figure 2(a), mathematical expression for I_{D1} and I_{D2} in Eq. (4) and Eq. (5), are considered.

$$I_{D1} = \int_0^{2\phi_{B,avg}} \rho I_{sat1} \left[\exp\left(\frac{qV_{D1}}{kT}\right) - 1 \right] d\phi_B \quad (4)$$

$$I_{D2} = \int_0^{2\phi_{B,avg}} \rho I_{sat2} \left[1 - \exp\left(-\frac{qV_{D2}}{kT}\right) \right] d\phi_B \quad (5)$$

T is temperature, q is the elemental charge and k is Boltzmann constant. I_{sat1} and I_{sat2} are saturation current at reverse bias for D1 and D2, respectively. The saturation current is given as follows.

$$I_{sat1} = a_1 A^{**} T^2 \exp\left(-\frac{q\phi_B}{kT}\right) \quad (6)$$

$$I_{sat2} = a_2 A^{**} T^2 \exp\left(-\frac{q\phi_B}{kT}\right) \quad (7)$$

a_1 and a_2 are area of Schottky electrode in D1 and D2, respectively. A^{**} is Richardson constant. Then, the BBSD current (I_{D1} and I_{D2}) is obtained by solving the simultaneous Eq. (1).

To compute the BBSD current in the device model B with no current spreading (Figure 2(b)), current in each parallel lines need to be solved before they can be added though integration. The used current density equation (J_{D1} and J_{D2}) for the parallel line is shown by Eq. (8) and Eq. (9).

$$J_{D1} = A^{**} T^2 \exp\left(-\frac{q\phi_B}{kT}\right) \left[\exp\left(\frac{qV_{D1}}{kT}\right) - 1 \right] \quad (8)$$

$$J_{D2} = A^{**} T^2 \exp\left(-\frac{q\phi_B}{kT}\right) \left[1 - \exp\left(-\frac{qV_{D1}}{kT}\right) \right] \quad (9)$$

The simultaneous equation that needs to be solved for each of the parallel lines is Eq. (10) and Eq. (11).

$$V_{D1} + V_{D2} + a_1 J_{D1} R - V_A = 0 \quad (10)$$

$$V_{D1} + V_{D2} + a_2 J_{D2} R - V_A = 0 \quad (11)$$

The BBSD current is obtained by using either J_{D1} or J_{D2} . Eq. (12) shows the solution using J_{D1} .

$$I = \int_0^{2\phi_{B,avg}} a_1 \rho J_{D1} d\phi_B \quad (12)$$

All the calculations were done using Python scientific programming software called Spyder. To check the validity of the solution, the final values of I_{D1} and I_{D2} are compared. Both should be identical as both diodes are connected in series.

3. Results and Discussion

In this work, the effect of standard deviation (σ_B) and temperature (T) to the current curve of the BBSD was investigated. Other device and material parameters are fixed (i.e. $a_1 = 10^{-6} \text{ cm}^2$, $a_2 = 10^{-4} \text{ cm}^2$, $\phi_{B,avg} = 0.5 \text{ eV}$ and $R = 100 \Omega$). The BBSD is assumed to be fabricated on silicon substrate (i.e. $A^{**} = 112 \text{ Acm}^{-2}\text{K}^{-2}$). Figure 3 shows the current curves with different σ_B values for model A plotted using Eq. (4) and Eq. (5), and model B using Eq. (2). The considered σ_B values were 5, 50, 100 and 250 meV. The smallest σ_B is equivalent to 1% of the mean barrier height. While the highest σ_B value is equivalent to 50% of the mean barrier height. Under the voltage application, the BBSD current is always limited by the Schottky junction that in reverse-bias condition [14]. At negative applied voltage, diode 1 is in reverse-bias condition. Thus, the device current is determined by diode 1. On the other hand, at positive voltage, diode 2 limits the device current as it is in reverse-bias condition. In ideal case where the barrier potential is homogenous, the saturation current of a Schottky diodes is calculated using Eq. (5) and Eq. (6). If the barrier height is 0.5 eV, the I_{sat1} and I_{sat2} are 4.16×10^{-8} and $4.16 \times 10^{-6} \text{ A}$, respectively. As shown in Figure 3(a) and Figure 3(b), in case of small barrier height variation, the obtained current is almost equivalent to the ideal case given as black solid line. The ideal case is where the no barrier height variation is considered. Model A and model B produced identical results.

As the σ_B increases, the current produced by both models increased. Here, number of sites (i.e. current path) with barrier potential lower than $\phi_{B,avg}$ becomes significant. Such sites or localities provide paths for current flow even at low applied voltage. This situation results in the reduction of the apparent barrier height ($\phi_{B,app}$). At higher σ_B , the discrepancy between results from model A and B becomes more pronounced. In general, model B (i.e. no current spreading) produced lower current values.

Apparent barrier height and ideality factor (n) can be extracted from the current curves in Figure 3 for further analysis. For simplification, the extraction was done only for diode 1 using procedure discussed in ref [14]. The resistance used in the device modelling is relatively low. Thus, the voltage drop at the series resistors can be ignored when determining apparent barrier height and ideality factor. At negative applied voltage, the BBSD current curve can be fitted to the following equation.

$$I = I_{sat1} \exp\left(\frac{qV}{nkT}\right) \left[1 - \exp\left(-\frac{qV}{kT}\right)\right] \quad (13)$$

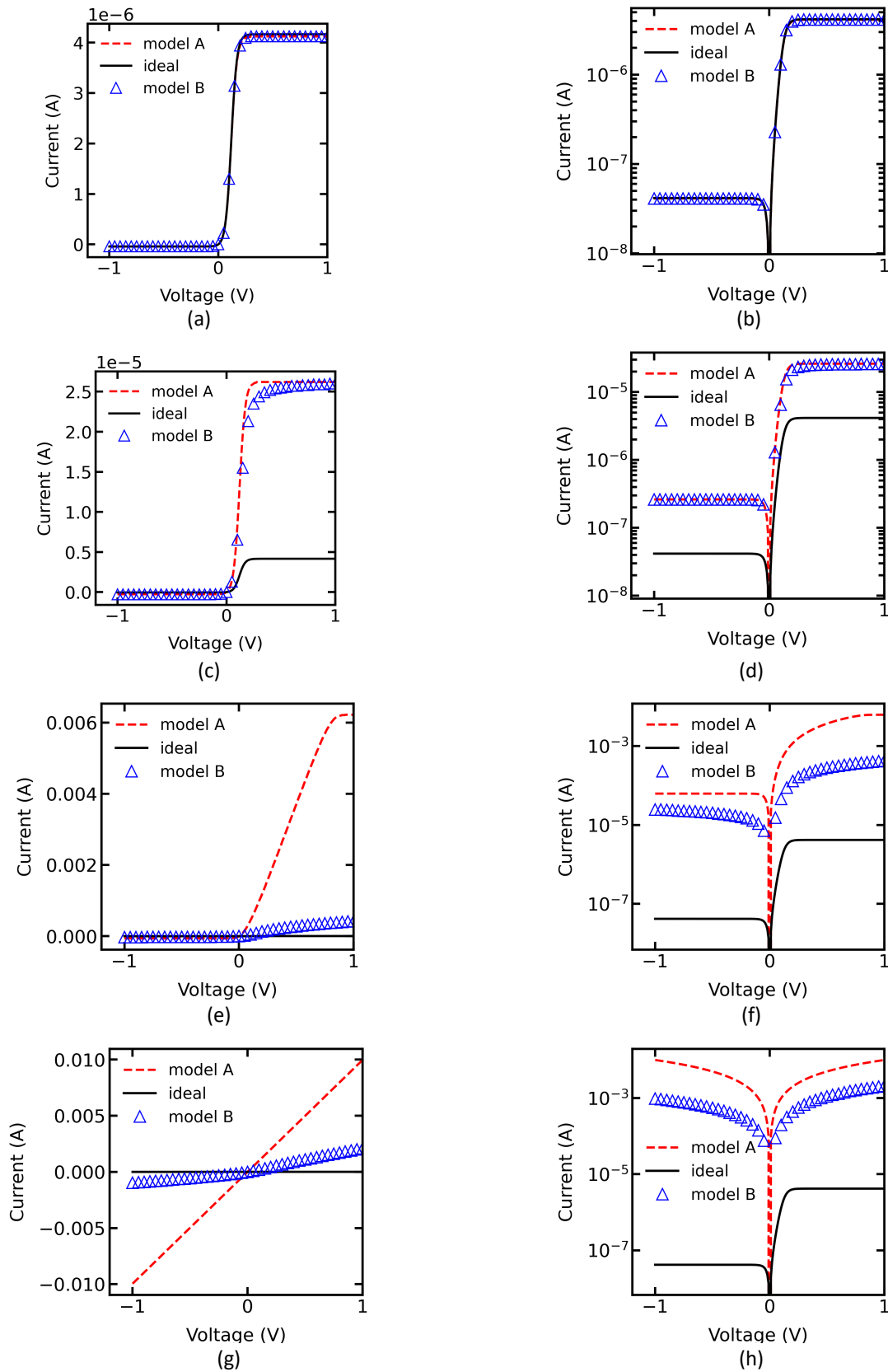


Fig. 3. Linear-scale and semi log plots of the current curves obtained using different σ_B . (a) and (b) $\sigma_B = 5$ meV, (c) and (d) $\sigma_B = 50$ meV, (e) and (f) $\sigma_B = 100$ meV, and (g) and (h) $\sigma_B = 250$ meV

The equation can be re-arranged to the following expression.

$$\ln\left(\frac{I}{1 - \exp\left(-\frac{qV}{kT}\right)}\right) = \ln(I_{sat1}) + \frac{qV}{nkT} \quad (14)$$

From the plot of $\ln\left(I/\left(1 - \exp\left(-\frac{qV}{kT}\right)\right)\right)$ versus V , n and I_{sat1} can be calculated. Apparent barrier height is computed from the I_{sat1} .

For the analysis of apparent barrier height and ideality factor, data for BBSD with $\sigma_B = 250$ meV was ignored. This is because the current curve largely deviated from the expected current curve of a BBSD device. Apparent barrier height could not be extracted from the linear current-voltage characteristic shown in Figure 3(g). Figure 4 shows the extracted n and $\phi_{B,app}$ as a function of the σ_B . As the standard deviation increases to 100 meV, the ideality factor for model B increases 2.6 %. As for model A, the increment of ideality factor was only 0.08 %. In comparison to model B, minimal change in ideality can be observed for model A. For device structure with complete current spreading, almost ideal thermionic transport is expected even when there is significant barrier fluctuation. Note that the discussed ideality factor is different with the ideality factor analyzed in a single Schottky diode [6]. The ideality factor defined in Eq. (13) influences the current curve at both forward and reverse bias. On the other hand, the typical ideality factor in a single Schottky diode only affects the forward-bias operation. A slight change in the ideality factor of the BBSD will lead to a marked change in the current curve. As for apparent barrier height, the result was as expected. Model A shows lower apparent barrier height with 37.8 % reduction at standard deviation of 100 meV. In case of model B, the reduction of apparent barrier height is 28.9 %.

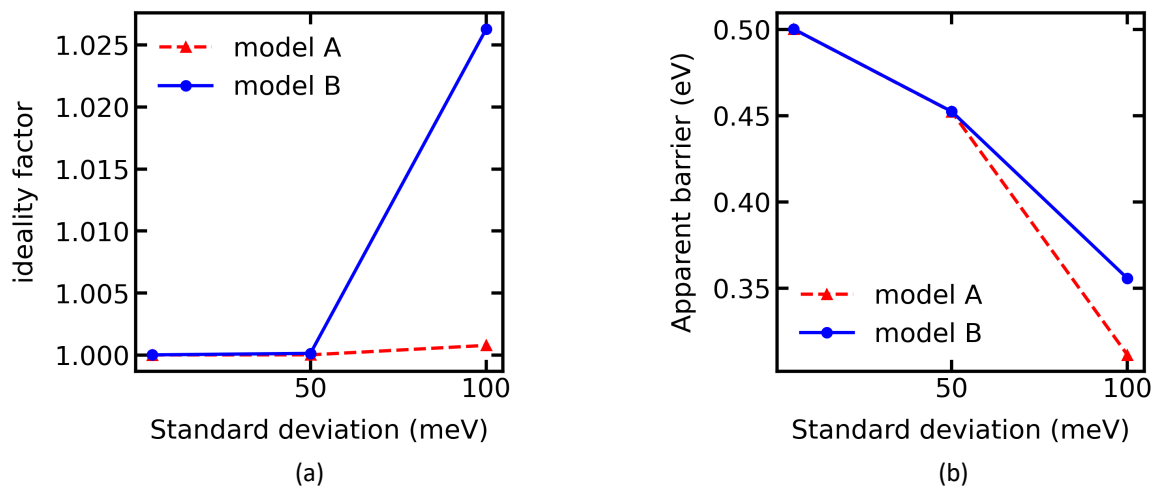


Fig. 4. (a) Extracted ideality factor (b) Apparent barrier height as a function of standard deviation

Next, the effect of the temperature to the current curve is investigated. Figure 5 shows the current curves simulated at four different temperature (250, 300, 350 and 400 K). The standard deviation was fixed at 50 meV in Figure 5(a). As the temperature increased, the current increased. There will be more electrons with higher energy that can overcome the barrier potential at the interface. For the produced current curve, the difference between model A and model B was not pronounced. The standard deviation of 50 meV is a small fluctuation. This result is consistent with

Figure 4. Figure 5(b) shows the temperature dependent current curves for standard deviation of 100 meV. Similar temperature effect could be confirmed. Pronounced difference between model A and B is due to the difference in apparent barrier height and ideality factor.

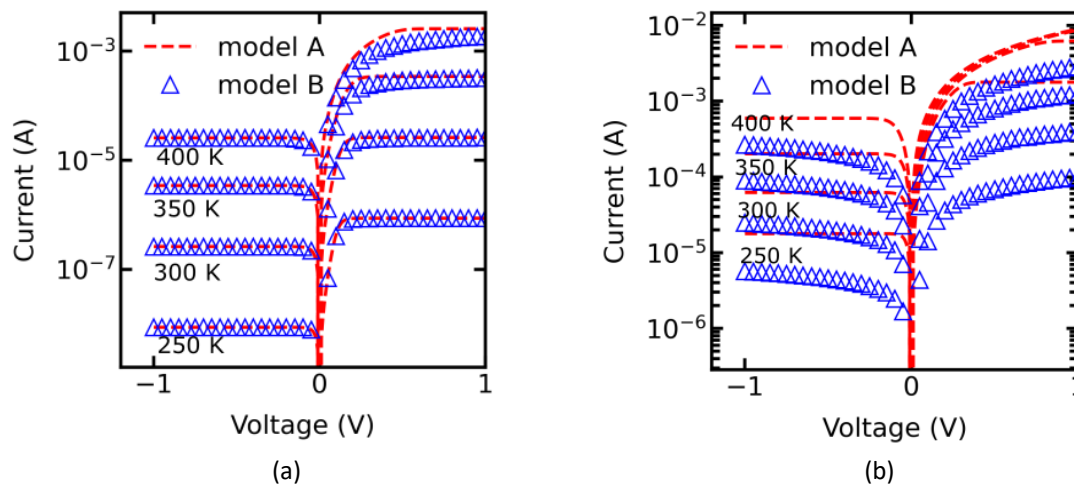


Fig. 5. Simulated current curve at different temperature (a) Standard deviation of 50 meV (b) Standard deviation of 100 meV

4. Conclusions

Two different device models of an inhomogeneous BBSD were considered and simulated. Based on the device modelling and simulation, the effect of current spreading, standard deviation of barrier height and temperature were analyzed and discussed. Under high barrier height fluctuation, device model without current spreading produced current curve that deviates from the ideal thermionic equation. This is shown by the change in ideality factors. As the standard deviation of barrier height increased, the current increased. The BBSD current also increased at the higher temperature. All the simulation results are consistent with the reported experimental works.

Acknowledgement

This work is financially supported by Universiti Teknologi Malaysia through UTM-FR research grant vot:22H16 and UTM-Tier 2 research grant vot. 16J02, and Malaysia General Service Division under HLP scholarship program.

References

- [1] Issa, Hanady H., Mahmoud S. Badran, Saleh M. Eisa, and Hani F. Ragai. "Low Power 7 nm FinFET based 6T-SRAM Design." *Journal of Advanced Research in Applied Mechanics* 42, no. 1 (2018): 12-17.
- [2] Mohamada, K. A., H. T. Hoh, B. K. Ghoshc, A. Aliasd, and I. Saade. "Fabrication and Characterization of Organic Transistors using Poly (triarylamine)-based Amorphous Semiconductor by Spin-coating Method." *Journal of Advanced Research in Applied Mechanics* 13, no. 1 (2015): 24 - 30.
- [3] E-Lin, Cindy Wong, WH Wan Hasanb, and S. Isaack. "The Design and Characterization of Breakdown Mechanism on P+/N-Well Single Photon Avalanche Diode (SPAD)." *Journal of Advanced Research in Applied Mechanics* 13, no. 1 (2015): 12 - 23.
- [4] Zhou, Feng, Weizong Xu, Fangfang Ren, Dong Zhou, Dunjun Chen, Rong Zhang, Youdou Zheng, Tinggang Zhu, and Hai Lu. "High-voltage quasi-vertical GaN junction barrier Schottky diode with fast switching characteristics." *IEEE Electron Device Letters* 42, no. 7 (2021): 974-977. <https://doi.org/10.1109/LED.2021.3078477>
- [5] Liu, Jielong, Minhan Mi, Jiejie Zhu, Pengfei Wang, Yuwei Zhou, Siyu Liu, Qing Zhu et al. "High-Performance AlGaIn/GaN HEMTs With Hybrid Schottky–Ohmic Drain for Ka-Band Applications." *IEEE Transactions on Electron Devices* 69, no. 8 (2022): 4188-4193. <https://doi.org/10.1109/TED.2022.3182294>

- [6] Chen, Duo, Wencheng Yu, Lin Wei, Jiasheng Ni, Hui Li, Yanxue Chen, Yufeng Tian, Shishen Yan, Liangmo Mei, and Jun Jiao. "High sensitive room temperature NO₂ gas sensor based on the avalanche breakdown induced by Schottky junction in TiO₂-Sn₃O₄ nanoheterojunctions." *Journal of Alloys and Compounds* 912 (2022): 165079. <https://doi.org/10.1016/j.jallcom.2022.165079>
- [7] Sze, Simon M., Yiming Li, and Kwok K. Ng. *Physics of semiconductor devices*. John Wiley & sons, 2021.
- [8] Wang, Zhiliang, Meiguang Zhu, Xuejiao Chen, Qiang Yan, and Jian Zhang. "Defect-assisted tunneling current-transport mechanism for Schottky diodes of Pt thin film on p-SiNWs tips." *Microelectronic engineering* 103 (2013): 36-41. <https://doi.org/10.1016/j.mee.2012.09.017>
- [9] Osvald, J. "Influence of lateral current spreading on the apparent barrier parameters of inhomogeneous Schottky diodes." *Journal of applied physics* 99, no. 3 (2006). <https://doi.org/10.1063/1.2169879>
- [10] Azmi, Siti Nadiah Che, Shaharin Fadzli Abd Rahman, Amirjan Nawabjan, and Abdul Manaf Hashim. "Junction properties analysis of silicon back-to-back Schottky diode with reduced graphene oxide Schottky electrodes." *Microelectronic Engineering* 196 (2018): 32-37. <https://doi.org/10.1016/j.mee.2018.04.020>
- [11] Hsieh, Cheng-Chih, Yao-Feng Chang, Ying-Chen Chen, Davood Shahrjerdi, and Sanjay K. Banerjee. "Highly non-linear and reliable amorphous silicon based back-to-back Schottky diode as selector device for large scale RRAM arrays." *ECS Journal of Solid State Science and Technology* 6, no. 9 (2017): N143. <https://doi.org/10.1149/2.0041709jss>
- [12] Labar, Rini, and Tapas Kumar Kundu. "Fabrication and Characterization of Back-to-Back Schottky Diode in Ni/ZnO/Ag Nanojunction." *Journal of Electronic Materials* 51, no. 1 (2022): 223-231. <https://doi.org/10.1007/s11664-021-09280-1>
- [13] Luo, Qian, Jiangfeng Du, Mohua Yang, Liangchen Wang, Tong Jin, and Qi Yu. "Back-to-back Schottky diode adopted for the measurement of GaN films and its Schottky contacts." *Semiconductor science and technology* 20, no. 6 (2005): 606. <https://doi.org/10.1088/0268-1242/20/6/021>
- [14] Averine, S., Y. C. Chan, and Y. L. Lam. "Evaluation of Schottky contact parameters in metal–semiconductor–metal photodiode structures." *Applied Physics Letters* 77, no. 2 (2000): 274-276. <https://doi.org/10.1063/1.126948>
- [15] Nouchi, Ryo. "Extraction of the Schottky parameters in metal-semiconductor-metal diodes from a single current-voltage measurement." *Journal of Applied Physics* 116, no. 18 (2014). <https://doi.org/10.1063/1.4901467>
- [16] Chiquito, Adenilson J., Cleber A. Amorim, Olivia M. Berengue, Luana S. Araujo, Eric P. Bernardo, and Edson R. Leite. "Back-to-back Schottky diodes: the generalization of the diode theory in analysis and extraction of electrical parameters of nanodevices." *Journal of Physics: Condensed Matter* 24, no. 22 (2012): 225303. <https://doi.org/10.1088/0953-8984/24/22/225303>
- [17] Mikhelashvili, V., R. Padmanabhan, and G. Eisenstein. "Simplified parameter extraction method for single and back-to-back Schottky diodes fabricated on silicon-on-insulator substrates." *Journal of Applied Physics* 122, no. 3 (2017). <https://doi.org/10.1063/1.4994176>
- [18] Wang, Zuo, Wanyu Zang, Yeming Shi, Xingyu Zhu, Gaofeng Rao, Yang Wang, Junwei Chu et al. "Extraction and Analysis of the Characteristic Parameters in Back-to-Back Connected Asymmetric Schottky Diode." *physica status solidi (a)* 217, no. 8 (2020): 1901018. <https://doi.org/10.1002/pssa.201901018>
- [19] Osvald, Jozef. "Back-to-back connected asymmetric Schottky diodes with series resistance as a single diode." *physica status solidi (a)* 212, no. 12 (2015): 2754-2758. <https://doi.org/10.1002/pssa.201532374>
- [20] Kim, Hyunsoo, Seong-Ju Park, and Hyunsang Hwang. "Effects of current spreading on the performance of GaN-based light-emitting diodes." *IEEE Transactions on Electron Devices* 48, no. 6 (2001): 1065-1069. <https://doi.org/10.1109/16.925227>